



# FEM-based thermal modelling of the cutting process using power law-temperature dependent concept

**W. Grzesik \***, **P. Niesłony**

Department of Manufacturing Engineering and Production Automation,  
Opole University of Technology, ul. St. Mikołajczyka 5, 45-271 Opole, Poland

\* Corresponding author: E-mail address: w.grzesik@po.opole.pl

Received 10.12.2007; published in revised form 01.02.2008

## ABSTRACT

**Purpose:** Purpose of this study is to compare two variants of the FEM simulation model of orthogonal cutting process of AISI 1045 carbon steel with uncoated and multilayer-coated carbide tools i.e. standard and Power Law-Temperature Dependent (PL-TD) options. The primary reason for undertaking this problem was unsatisfactory accuracy of the predictions of cutting temperature especially for coated cutting tools.

**Design/methodology/approach:** Methodology used employs the Lagrangian-FEM model with more accurate thermophysical properties of the substrate and coating materials. All thermal properties (thermal conductivity and diffusivity and specific heat) are expressed in the forms of polynomial models of the 5th degree. Multi-layer coating is substituted by homogeneous monolithic layer with equivalent thermal properties. In addition, these simulation algorithms use the Johnson-Cook constitutive law.

**Findings:** Basically, the FEM package applied allows the temperature distribution and heat flux intensity to be predicted closer to appropriate measurements and computations.

**Research limitations/implications:** Research limitations deal with the lack of reliable data and models for both cutting tool and workpiece material. Future research should be focused on other coatings which are commonly used in cutting tool industry.

**Practical implications:** They can be related to more detailed inputs from research and developing centers which exist in many leading branches of industry. Unfortunately, academic approach is sometimes very narrow and does not consider real machining conditions.

**Originality/value:** Originality of this simulation approach can be seen in elaborating more accurate models for thermal properties. Moreover, it contributes to finding some fundamental relationships between all physical phenomena involved into tool-chip contact behaviour.

**Keywords:** Tool materials; Machining; Thermal behaviour; FEM simulation; Coatings

## METHODOLOGY OF RESEARCH, ANALYSIS AND MODELLING

### 1. Introduction

In order to implement a range of advanced machining technologies, including especially high-speed and dry or near dry processes, modern machine shops employ cutting tools treated with more sophisticated coatings [1]. Moreover, machining

operations are tested by means of engineering simulation tools, mainly based on the Finite Element Method (FEM). Unfortunately, until now a few FEM-based simulation techniques (Lagrangian, Eulerian, ALE) used are not able to model integrally all physical phenomena involved into complex machining process with demanded engineering accuracy [2]. The barriers in

developing more effective FEM algorithms are insufficient mechanical and thermo-physical data on both workpiece and cutting tool materials. The thermal modelling is a bottleneck of FEM simulation due to uncertainties in arbitrary using such inputs as heat partition coefficient, friction coefficient and both thermal conductivity and diffusivity. Some successful initiatives regarding multilayer coatings deal with such specific aspects as: thermal-dependent physical properties [3], composite layer concept [4], thermal constriction resistance phenomenon [5], uncertainties in material data and its effect on the discrepancies between modelled and IR-measured temperatures [6], heat transfer in various domains of time [7], tool-chip interfacial friction models [8], the global heat transfer coefficient in ALE formulation [9] and the inverse identification algorithm for flow stress data [10]. In this paper, the updated thermal properties of WC-6%Co substrate and multilayer CVD-TiC/Al<sub>2</sub>O<sub>3</sub>/TiN coating system, were implemented into the Lagrangian-FEM model.

## 2. Experimental program

### 2.1. Determination of thermophysical properties of cutting tool materials

In this study, the temperature-dependent thermal conductivity  $\lambda(t)$  was determined by prior measuring the thermal diffusivity ( $\alpha$ ) and the specific heat ( $c_p$ ), all as functions of temperature. In addition, three layer coating was replaced by a homogeneous layer with equivalent thermal properties (curve 3L in Fig. 1) described previously in Refs. [4] and [12-15]. Relevant equations for ISO P20 carbide tools elaborated on literature data are as follows:

$$\lambda = 33,34 + 0,01863 * t - 5,7449 * 10^{-6} * t^2 \quad (1a)$$

$$\alpha = 3,574 * 10^{-5} - 1,410 * 10^{-7} * t + 5,667 * 10^{-10} * t^2 - 1,1594 * 10^{-12} * t^3 + 1,128 * 10^{-15} * t^4 - 4,149 * 10^{-19} * t^5 \quad (1b)$$

$$c_p = 173,524 + 0,34528 * t - 0,00072486 * t^2 + 8,57275 * 10^{-7} * t^3 - 4,9327 * 10^{-10} * t^4 + 1,087713 * 10^{-13} * t^5 \quad (1c)$$

Adequate equations determined for composite coating are:

$$\lambda = 26,222 - 0,005542 * t - 2,472 * 10^{-5} * t^2 + 1,765 * 10^{-8} * t^3 \quad (2a)$$

$$\alpha = 8,9048 * 10^{-6} - 9,6314 * 10^{-9} * t - 7,0743 * 10^{-12} * t^2 + 1,9974 * 10^{-14} * t^3 - 8,2037 * 10^{-18} * t^4 \quad (2b)$$

$$c_p = 577,615 + 1,7261 * t - 0,00372 * t^2 + 4,2384 * 10^{-6} * t^3 - 2,376402685 * 10^{-9} * t^4 + 5,25656 * 10^{-13} * t^5 \quad (2c)$$

Fig. 1 presents the dependence of the thermal conductivity on temperature for all cutting tool materials considered, as well as AISI 1045 steel being the workpiece material.

### 2.2. Input data to the FEM simulation package

In this study, an updated Lagrangian finite element formulation is used to predict the thermal behaviour in orthogonal cutting of AISI 1045 medium carbon steel with P20 uncoated and CVD-TiC/Al<sub>2</sub>O<sub>3</sub>/TiN coated tools. Both standard and PL-TD material models available in the FEM software named *AdvantEdge* [11] were used. The PL-TD approach uses also the standard Johnson-Cook constitutive model but the user can vary

thermal conductivity, specific heat and thermal diffusivity as functions of temperature (Eqns. 1a-1c and 2a-2c).

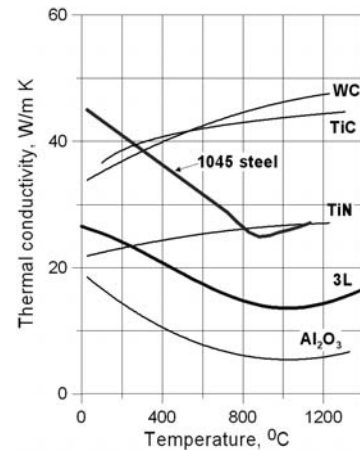


Fig. 1. Thermal conductivity of tool (substrate, coatings) and workpiece materials vs. temperature

Other inputs were values of the friction coefficient (0.631, 0.577 and 0.508 for P20 carbide tools and 0.676, 0.605 and 0.515 for 3L-coated tools) obtained experimentally for the three cutting speeds selected (103.2, 206.4 and 330 m/min) and feed rate of 0.16 mm/rev. It tends to be close to 0.5 at  $v_c=330$  m/min, which corresponds to the Coulomb friction model.

## 3. Experimental results and discussion

### 3.1. Cutting temperature

Comparison of the predicted and measured values of the average tool-chip temperatures for uncoated and coated tools and three selected cutting speeds are shown in Fig. 2.

### 3.2. Distribution of temperature at the tool-chip contact zone

The temperature distributions along the tool-chip interface and beneath the rake face at the point of peak temperature (at a distance of 0.2 mm from the cutting edge) predicted for different simulation conditions are shown in Figs. 3 and 4 respectively. It is evident from Fig. 3a that the standard FEM simulation generates temperature distribution curves with distinct peaks, which are localized at a constant distance of 0.15-0.25 mm from the cutting edge. For the PL-TD option a small plateau in the 0.2 mm wide area is a characteristic feature of these distributions. It should also be noticed that shorter distance from the cutting edge to the point with temperature stabilization was observed for coated tools. These findings are well supported by the magnitude of the reduced von Mises stresses acting on the rake face (9000 MPa vs. 4500 MPa) shown as zone I in Fig. 5. The zone Ia can be referred to the seizure region with intensive adhesive interaction. In addition, the boundary between the first (I) and second (II) zones coincides with the points of maximum interface temperatures.

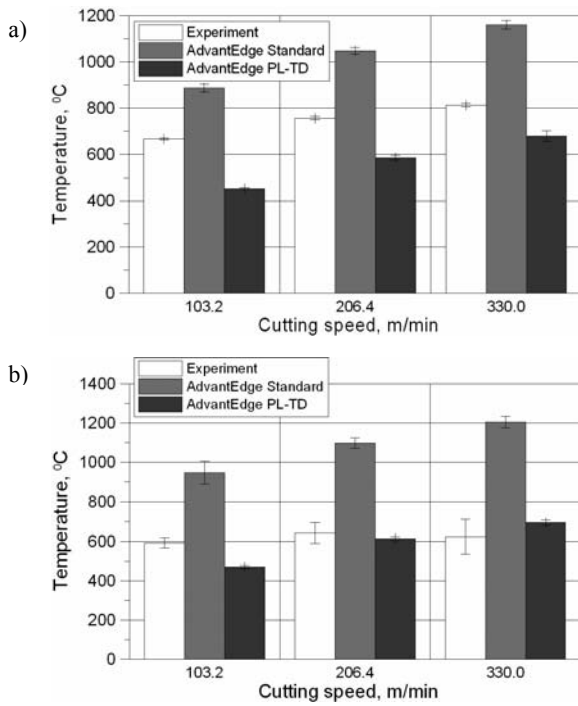


Fig. 2. Comparison of the measured cutting temperatures with FEM simulated values for ISO P20 carbide(a) and 3L coating (b)

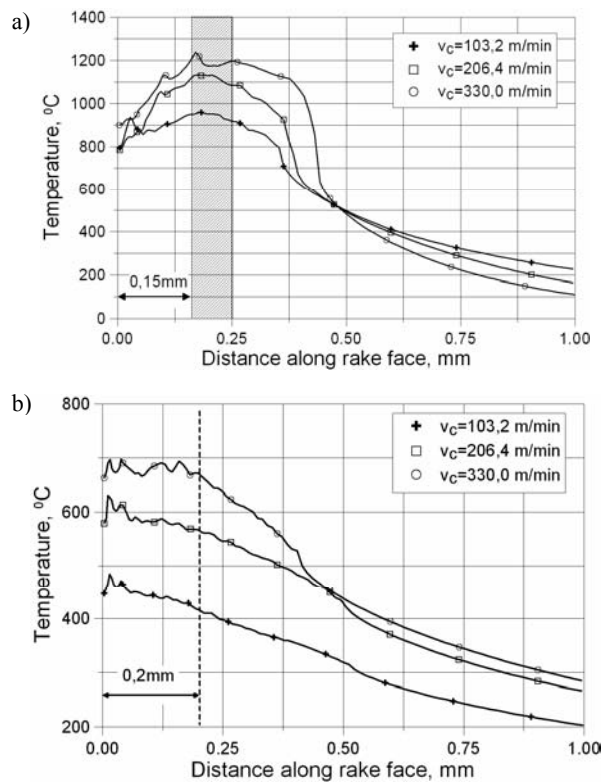


Fig. 3. Temperature distribution along rake face vs. cutting speed for AISI 1045 carbon steel and 3L coated tools: a) standard FEM; b) PL-TD

In general, the “standard” simulation provides substantially higher temperatures in comparison with thermocouple-based measurements. Better agreement was achieved in the PL-TD option and especially in case of coated tools for higher speeds, i.e. 200-330 m/min range.

The influence of the three layer coating on the temperature distribution beneath the tool-chip interface can be assessed based on the confrontation of the relevant distribution curves shown in Figs. 4a and 4b.

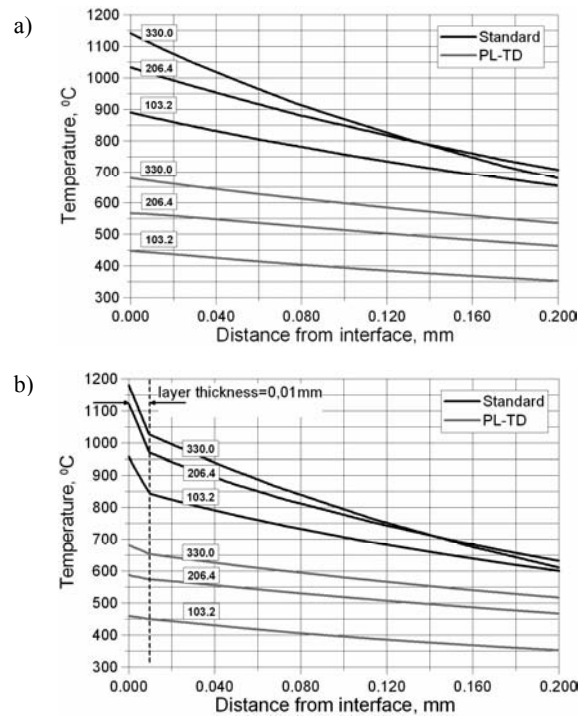


Fig. 4. Temperature distribution below the rake face in the point of maximum contact temperature for AISI 1045 steel and P20 carbide (a) and 3L coated (b) tools

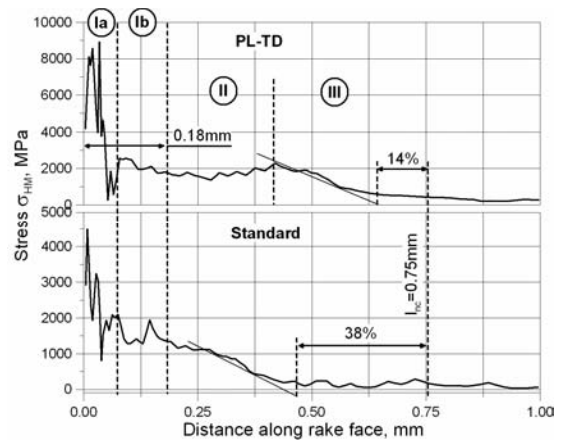


Fig. 5. Distribution of the reduced von Mises stress along rake face for AISI 1045 steel and 3L coated tools ( $v_c=103.2$  m/min)

For uncoated tools (Fig. 4a), temperatures decrease monotonically and the temperature gradients vary between 470-720 °C/mm. They are practically the same regardless of the simulation option employed. In contrast (Fig. 4b), for coated tools and the cutting speed of 330 m/min, this gradient reaches about 3000 °C/mm (equivalently 3.0 °C/μm) which documents well the thermal barrier effect caused by the Al<sub>2</sub>O<sub>3</sub> ceramic interlayer. As a result, the heat penetration effect in this thin layer is four times less than for uncoated carbide tools applied.

### 3.3. Visualization of thermal behaviour of the cutting zone

Some characteristic temperature maps covering the primary (PDZ) and secondary (SDZ) deformation areas obtained for different thermophysical data are shown in Fig. 6. In case of the PL-TD variant (Fig. 6b) the chip is visibly thicker and the field of higher temperatures is more extended in the chip. On the other hand, the maximum temperatures of about 600°C are localized closer to the cutting edge and the tool contact area is cooler (about 450°C). For example, the relevant temperature recorded for “standard” simulation (Fig. 6a) are equal to 880°C and 830°C, respectively.

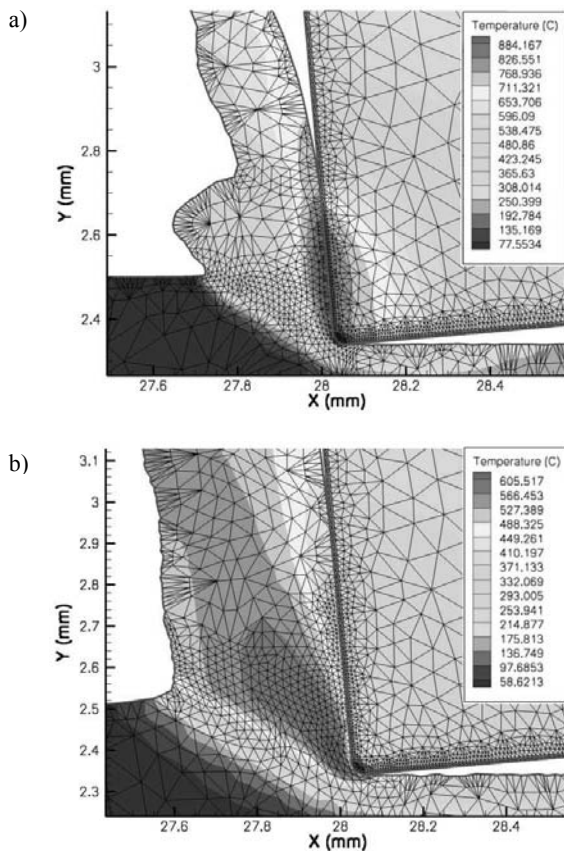


Fig. 6. Thermal maps for AISI 1045 carbon steel and 3L coated tools: a) standard FEM; b) PL-TD option ( $v_c=103.2$  m/min)

## 4. Summary

- i) Simulation option and input thermophysical data of the tool materials are decisive factors in obtaining proper temperature values in both primary and secondary deformation zones.
- ii) For 3L coated tools the best coincidence of experimental and modelled temperatures were obtained for PL-TD option and composite coating which represents “micro” approach to thermal functions of the coating deposited.
- iii) Temperature distribution patterns have some visible physical analogies to the reduced von Mises stresses and tool-chip contact behaviour.
- iv) The differences in thermal behaviours of uncoated and coated tools can be related to the intensity and fluctuation of the heat fluxes in the seizure region.

## References

- [1] F. Klocke, T. Krieg, Coated tools for metal cutting-features and applications, *Annals of the CIRP* 48/2 (1999) 515-525.
- [2] T.H.C. Childs, K. Maekawa, T. Obikawa, Y. Yamane, *Metal Cutting. Theory and Applications*, Arnold, London, 2000.
- [3] W. Grzesik, An investigation of the thermal effects in orthogonal cutting associated with multilayer coatings, *Annals of the CIRP* 50/1 (2001) 53-56.
- [4] W. Grzesik, Analytical models based on composite layer for computation of tool-chip interface temperature in machining steels with multilayer coated cutting tools, *Annals of the CIRP* 54/1 (2005) 91-94.
- [5] M.H. Attia, L. Kops, A New approach to cutting temperature prediction considering the thermal constriction phenomenon in multi-layer coated tools, *Annals of the CIRP* 53/1 (2004) 47-52.
- [6] M.A. Davies, Q. Cao, A.L. Cooke, R. Ivester, On the measurement and prediction of temperature fields in machining AISI 1045 steel, *Annals of the CIRP* 52/1 (2003) 77-80.
- [7] J. Rech, J.L. Battaglia, A. Moisan, Thermal influence of cutting tool coatings, *Journal of Materials Processing Technology* 159 (2005) 119-124.
- [8] T. Özel, The influence of friction models on finite element simulation of machining, *International Journal of Machine Tools and Manufacture* 46 (2006) 518-530.
- [9] E. Ceretti, L. Filice, D. Umbrello, F. Micari, ALE simulation of orthogonal cutting: a new approach to model heat transfer phenomenon at the tool-chip interface, *Annals of the CIRP* 56/1 (2007) 69-72.
- [10] J. Pujana, P.J. Arrazola, R.M.M. Saoubi, H. Chandrasekaran, Analysis of the inverse identification of constitutive equations applied in orthogonal cutting process, *International Journal of Machine Tools and Manufacture* 47 (2007) 2153-2161.
- [11] *Third Wave AdvantEdge 2D User's Manual, Version 5.0*, Minneapolis, USA, 2006.
- [12] W. Grzesik, M. Bartoszuk, P. Nieslony, Finite Element Modelling of temperature distribution in the cutting zone in turning process with differently coated tools, *Journal of Materials Processing Technology* 164-165 (2005) 1204-1211.
- [13] W. Grzesik, P. Nieslony, Physics based modelling of interface temperatures in machining with multilayer coated tools at moderate cutting speeds, *International Journal of Machine Tools and Manufacture* 44 (2004) 889-901.
- [14] W. Grzesik, M. Bartoszuk, P. Nieslony, Finite Element Modelling of temperature distribution in the cutting zone in turning process with differently coated tools, *Proceedings of the 13<sup>th</sup> Scientific International Conference „Achievements in Mechanical and Materials Engineering” AMME'2005, Gliwice-Wisla, 2005*, 259-262.
- [15] W. Grzesik, Composite layer-based analytical models for tool-chip interface temperatures in machining medium carbon steels with multi-layer coated cutting tools, *Journal of Materials Processing Technology* 176 (2006) 102-110.